Agent-based modelling of climate impacts at the global scale

Preliminary version, do not distribute without prior authorisation

Antoine Mandel*

May 13, 2023

Abstract

JEL Classification: D85, C65, D83

Keywords: climate impacts, integrated assessment, production networks, supply chains.

1 Introduction

Global warming will lead to increasing frequency, severity and duration of multiple climate hazards [1]. Direct impacts of these hazards on large firms can have substantial macro-economic consequences [2]. Additionally, the propagation of these impacts through global supply chains [3, 4] can significantly amplify macro-economic volatility [5, 6]. These evidences on the micro-economic origins of macro-economic volatility and the heterogeneity of the spatial distribution of hazards suggest that the macro-economic consequences of global warming should be evaluated from the bottom-up by considering impacts on individual production units and their propagation through production networks before aggregating at the macro level [7, 8]. Furthermore, the economic and policy relevance of low probability/high-impact events [9, 10] imply that one shall consider the whole distribution of risks rather than focus on their expected value. Co-occurring events resulting in compounding and cascading risks are particularly relevant in this respect [1, 11].

Against this background, existing approaches to climate impact assessment rely on a number of intermediary aggregation steps that can opacify transmission mechanisms, render difficult the identification of the main sources of risk (both in terms of exposure and hazards), underestimate the amplification of impacts through economic networks, and mostly fail to consider the tail fo the distribution of impacts. Indeed, optimal growth integrated assessment models [12, 13, 14] postulate the existence of a deterministic damage function that measure directly macro-economic impacts as a function of temperature. Computable general equilibrium models aggregate uncertainty and spatial heterogeneity

*antoine.mandel@univ-paris1.fr, Centre d'Economie de la Sorbonne, Paris School of Economics, Université Paris 1 Panthéon-Sorbonne and Climate Finance Alpha

as they consider expected value of impacts at the country or regional level [15, 16]. They also smoothen the response of the economy by considering it adjusts instantaneously and efficiently to impacts. The few existing agent-based approaches to integrated assessment [17, 18] allow to consider richer economic dynamics but also rely on aggregate representation of impacts and/or of economic units and do not yet match the empirical breadth of computable general equilibrium models.

This paper provides, to our knowledge, the first empirically calibrated firm-level agent-based model of the world economy. This model is matched with granular projections of climate impacts in order to project a complete distribution of macro-economic impacts, to identify structural changes in macro-economic volatility and and to pin down the main sources of risk, in terms of hazard, exposure and propagation channels . We account for the following set of hazards: tropical storms, winter storms, coastal flooding, river flooding, wildfires, heat stress, landslides, and agricultural droughts .

Our approach relies on a number of methodological and conceptual innovations. First, we have developed a simple agent-based model of economic dynamics that can simulate efficiently up to millions of firms, reproduce key stylized facts of economic dynamics and has a limit behavior consistent with equilibrium [19, 20, 21]. We can thus use the equilibrium state to calibrate the model while overcoming the computational [22] and conceptual [7, 8] limits of equilibrium models using agent-based dynamics. In particular, our model allows to account for supply bottlenecks, rationing, delays in price and behavioral adjustment that reduce the efficiency of the economic response to climate impacts with respect to equilibrium behavior. Second, we build on network reconstruction methods [23] to infer firm level production networks from global input-output tables [24] and large databases of firm-level characteristics. This allows to overcome limited availability of data about supply relationships and to generate firm-level networks consistent with global flows at the sectoral level. Third, the firm/plant level resolution of the model allows to represent climate impacts at a high level of spatio-temporal granularity and to account for compounding effects linked to the simultaneous occurrence of multiple hazards.

The remaining of this paper is organized as follows. Section 2 presents the key characteristics of our agent-based model and of the representation of climate impacts in a dynamics setting. Section 3 highlights the main quantitative results of our analysis . Section 4 impacts of climate hazards on economic dynamics. Section 4 provides a detailed description of our methods. Section 5 concludes.

2 An agent-based integrated assessment model

We model the global economy as a set $\mathcal{M}$ of 100088 agents consisting in a set $\mathcal{F}$ of 100000 geolocalized firms distributed across 44 world regions, and a set $\mathcal{H}$ of two representative households per region (see methods for details). TODO sectoral characteristics. Each firm produces a differentiated good using, as intermediary inputs, goods produced by other firms (from inside and outside the region) as well as labor and capital services (from the region). In each region, one household, referred to as worker, provides labor services and a second household, referred to as capitalist, provides capital services. Both households consume goods produced by firms (from inside and outside the region).

More formally, we consider discrete period of time $t = 1, \cdots, T$ and assume the state of each agent $i \in \mathcal{M}$ in each period $t \in N$ is characterized by (i) its stock of output $q_i^t \in \mathbb{R}_+$, (ii) the price of its output $p_i^t \in \mathbb{R}_+$ and (iii) its monetary balances $m_i^t \in \mathbb{R}_+$. The interactions in the economy are governed by the network of supply relationships represented by the column-stochastic matrix $\Phi^t = (\phi_{i,j}^t)_{i,j \in \mathcal{M}}$ where $\phi_{i,j}^t \in \mathbb{R}_+$ is the share of input i in the production/consumption process of agent j. In absence of external (climate-related) shocks, we assume that the evolution of the system is governed by the following agent-based dynamics.

1. Each agent $i \in \mathcal{M}$ receives the nominal demand $\sum_{j \in \mathcal{M}} \phi_{i,j}^t m_j^t$.

2. Agents adjust their prices frictionally towards their market-clearing values according to:
$$p_i^t = \tau_p \overline{p}_i^t + (1 - \tau_p) p_i^{t-1} \tag{1}$$
where $\tau_p \in [0, 1]$ is a parameter measuring the speed of price adjustment and $\overline{p}_i^t$ is the market-clearing price given by:
$$\overline{p}_i^t = \frac{\sum_{j \in \mathcal{M}} \phi_{i,j}^t m_j^t}{q_i^t}. \tag{2}$$

3. Agents receive inputs proportional to their demand (including proportional rationing in case of excess demand), i.e. the input of agent i in good j is given by:
$$x_{j,i}(t) = \min(q_j^t, \textstyle\sum_{k \in \mathcal{M}} a_{j,k}^t m_k^t / p_j^t) \phi_{j,i}^t \frac{m_i^t}{p_j^t} \tag{3}$$

4. Firms update their inventory by producing new output and accounting for sales, i.e:
$$q_i^{t+1} = q_i^t - \sum_{k \in \mathcal{M}} x_{i,k} + f_i(x_i) \tag{4}$$
where f_i is firm i production function (see methods).

5. The inventory of "households" is set equal to their (fixed) supply of labor and capital services.

6. Money balances are determined by expenses and revenues, i.e:
$$\forall i \in M, \; m_i^{t+1} = m_i^t + \sum_{k \in M} p_i^t x_{i,k}^t - \sum_{k \in M} p_k^t x_{k,i}^t \tag{5}$$

7. Firms adjust frictionally their input share:
$$\phi_{\cdot,i}^{t+1} = \tau_w \overline{\phi}_{\cdot,i}^t(p^t) + (1 - \tau_w) \phi_{\cdot,i}^t \tag{6}$$
where $\tau_w \in [0, 1]$ measures the speed of technological adjustment and $\overline{\phi}_{\cdot,i}^t(p^t)$ is the optimal input combination given prevailing prices (see methods for details).

The behavior of this model has been extensively analyzed in previous contributions [19, 21]. If price adjustment is fast, the economy converges to the underlying general equilibrium (see methods). If price adjustment is slow, inventories carry the burden of adjustment and the economy is characterized by a synchronized state with large "cyclical volatility". The application of the model to the assessment of COVID lockdown policies has highlighted that the consideration of dynamic propagation mechanisms, through the network of supply relationships Φ, allows to represent more precisely the recovery period. Furthermore, even in the parameter range where general equilibrium is dynamically stable, cost estimates are much larger if one accounts for out-of-equilibrium adjustments than in computational general equilibrium models [25, 20].

The model provides a dynamic, micro-level and geolocalized representation of the production and exchange processes. This is a natural framework to assess climate impacts from the bottom-up. Conceptually, the state of the climate can be seen as a stochastic process whose realisations impact the local supply of labor and capital services in the economy. More formally, one considers a family of stochastic processes $(\lambda_i^t)_{i\in\mathcal{N}}$ and $(\kappa_i^t)_{i\in\mathcal{N}}$, with values in $[0,1]$, representing the availability of labor and capital services at the location of firm i. An amount $x^t_{\ell(i),i}$ of labor input purchased by firm i in period t then effectively yield $\lambda_i^t x^t_{\ell(i),i}$ units of labor services and, similarly, an amount $x^t_{k(i),i}$ of labor input purchased by firm i in period t effectively yield $\kappa_i^t x^t_{k(i),i}$ units of capital services. Our actual model of climate impact specifies (i) how the stochastic processes defining local impacts on labor and capital services are derived from projections of future climate and extreme weather events, (ii) how economic agents react to these direct impacts and (iii) how they propagate through input-output relationships (indirect impacts).

As for the modelling of direct impacts, lacking a comprehensive understanding of the correlation structure across space, time and type of hazards, the existing literature has partitioned climate impacts in (independent) domains/hazards and usually considers the year as a reference timeframe. Thus hazards are usually characterized by their yearly probability of occurrence or their return periods (in years) while the occurrence of hazards is assumed to be independent across years (though generally not identically distributed to account for the effects of climate change). In relation to this literature, we consider the following set $\mathcal{H}$ of hazards/domains: tropical storms, winter storms, coastal flooding, river flooding, wildfires, heat stress, landslides, and agricultural droughts . We then fix a time frame (between 2020 and 2090) and a climate scenario (among RCP 2.6, RCP 6 and RCP 8.5) and generate realisations of climate impacts according to the following procedure (see methods for details).

- For each year of the time-frame, we draw a yearly realization of each hazard for each location according to the distribution corresponding to the given year and climate scenario.

- We further draw uniformly at random (within the potential period of occurrence) the starting date of the hazard.

- Realizations can be correlated across hazards and locations because they are induced by the same event (e.g. a tropical storm yielding wind and flood related impacts at multiple contiguous locations) or because they are driven by the same climatic conditions, (e.g. agricultural droughts and heat-stress driven by the same temperature and precipitation patterns).

- For each realized hazard and each agent i, we use vulnerability functions taking into account the intensity of the hazard at the location of i as well as the the technological and geographical characteristics of i to determine the impact on labor and capital services.
- As for impact on labor services, they are directly derived from the vulnerability function, which is conventionally expressed in terms of reduced labor productivity. The factor λ_i^t then corresponds to the reduced productivity level during the occurrence of the hazard.
- As for impact on capital, services, vulnerability metrics are usually expressed in terms of share of capital destroyed. Therefrom, one can also derive number of business days interruptions (see methods for details). To represent the impacts an hazard occurring at date t_0 inducing the loss of a share k_i of capital and d_i days of business to agent i, we use two possible specifications for κ_i^t :
  - A 0-1 specification whereby $\kappa_i^t = (1 - k_i)$ for $t \in [t_0, t_0 + d_i]$
  - A linear specification whereby $\kappa_i^t = 1 - k_i \frac{t_0 + d_i - t}{d_i}$ for $t \in [t_0, t_0 + d_i]$
- If multiple hazard co-occur at the same location, the maximum of impacts is taken into consideration to define κ_i^t and λ_i^t.

The direct impact of these climate shocks on the dynamics of the model is the distortion of labor and capital supply so that Equation (4) above is perturbed as:

$$q_i^{t+1} = q_i^t - \sum_{k \in \mathcal{M}} x_{i,k}^t + f_i(\lambda_i^t x_{\ell(i),i}^t, \kappa_i^t x_{k(i),i}^t, x_{-\{\ell(i),k(i)\},i}^t) \tag{7}$$

The firm has limited capacity to adapt to these direct impacts on capital and labor services by substituting other inputs (following Equation (6)) as the elasticity of substitution between labor services, capital services and intermediary inputs is low (less than one in our setting with nested Cobb-Douglas structure, see methods). Thus, the firm is likely to face substantive reduction of its output when experiencing a climate hazard.

Following Equations (2) to (4), this shock propagates downstream in the production networks as firms sequentially receive less intermediary inputs and thus produce less output. These reductions in output lead to a combination of rationing and upward price adjustment proportionally to the speed of price adjustment. In turn, following Equation (6), upward price adjustments can lead downstream firms to substitute away from impacted firms and thus to reduce their nominal demand. This feedback effect can then propagate upwards as, following Equation (5), affected firms themselves reduce their nominal demand.

3 Results

We provide preliminary results highlighting the impact of climate shocks on the dynamics of output. We consider climate impacts corresponding to scenario RCP 2.6 at the horizon 2050. Figure 1 displays the resulting trajectories of 20 Monte-Carlo runs for random draws of impacts according to the corresponding distribution of climate impacts.

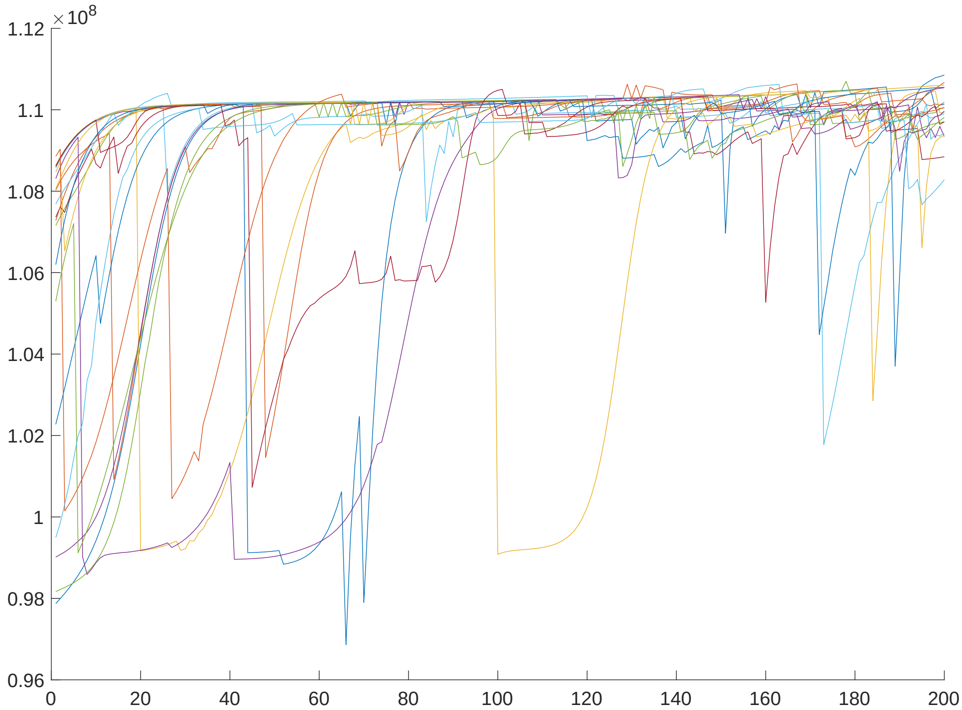

Figure 1: Trajectory of aggregate output of the economy for 20 random realizations of climate impacts

4 Methods

4.1 Calibration of the production network

We generate a global firm-level production network by combining the world input-output database [WIOD, see 26] with Capital IQ global firms database [CIQ, see 27] as follows. The WIOD is based on a taxonomy of 56 sectors from the International Standard Industrial Classification revision 4 (ISIC Rev. 4) and 44 countries (EU 27 countries, Australia, Brazil, Canada, China, India, Indonesia Japan, Mexico, Norway, Russia, Taiwan,Turkey, South Korea, Switzerland, United Kingdom, United States, and the rest of the world). It provides for each such country/sector pair, the value of input-output flows, the labor and capital share in value-added and the final consumptions. We further introduce two representative "households" per country: a "worker" receiving from each domestic sector the labor share of value-added and consuming proportionally to final consumption, a "capitalist" receiving from each domestic sector the capital share of value-added and consuming capital formation and the residual share of consumption. The WIOD thus induces a production network with $N^0 = 2552$ agents (corresponding to 56 productive sectors and 2 household sectors per country) whose interactions are a characterized by a matrix A^0 such that $A^0_{i,j}$ represents the input flow from agent i to agent j. For each agent i, the sum of coefficient on line i, $\sum_{j=1}^{N^0} A^0_{i,j}$, that represents the total revenues is equal to the sum of coefficient on column i, $\sum_{j=1}^{N^0} A^0_{j,i}$, that represent total expenditures.

CIQ is a global database of firms. After filtering our for firms for which data is available on revenues, number of employees, industrial sector (sic code), country and address, we obtain a total of 644782 firms. This sample appears representative as it accounts for 100 trillions US$ in revenues (out of a total world output of 240 trillions US$ according to WIOD) and for 300 million of employees [out of 1.3 billion people employed in the formal sector according to 28]. We thus use the CIQ database to downscale the WIOD production network at the firm-level, generating a production network with $N = 6$ (the set of CIQ firms and two representative households per WIOD country as above). The downscaling procedure is as follows.

(i) We first match each firm in CIQ to the corresponding country/sector pair in WIOD. We then assign to each firm a level of output corresponding to the share of the output of the WIOD country/sector pair given by the ratio between its revenues and the total revenues of the firm matched to that country/sector pair.

(ii) For each household h , we draw at random $\deg_h$ firms ($\deg_h = 200$ by default) that belong to country-sector pairs ℓ such that $A^0_{\ell,h} > 0$ and allocate the value of the consumption of h uniformly among those (up to the level of output they have available).

(iii) To each firm j in a country-sector pair k, we assign a share of the labor and capital compensation paid by k to the worker and the capitalist in its country (denoted respectively $w(j)$ and $c(j)$). proportional to its share of revenues Further, we draw at random $\deg_j$ firms ($\deg_j = 20$ by default) that belong to country-sector pairs ℓ such that $A^0_{\ell,k} > 0$ and allocate the value of the intermediary consumption of j (i.e. the value of its output minus the payment for the compensation of labor and capital) uniformly among those (up to the level of output they have available).

(iv) The resulting matrix of input-output flows A^1 is not necessarily consistent in the sense that one might have $\sum_{j=1}^{N} A^1_{i,j} \neq \sum_{j=1}^{N} A^1_{j,i}$. To make it consistent, we first derive a matrix of input requirement by normalizing A^1 to $\underline{A}^1$ defined for all i, j by $\underline{A}^1_{i,j} = A^1_{i,j} / \sum_{k=1}^{N} A^1_{k,j}$. The matrix $\underline{A}^1$ is column-stochastic and the associated Perron-Froebenius eigenvector v represents the distribution of output among firms when production occurs according to the input requirements specified by $\underline{A}^1$. We then rescale the matrix proportionally to total output in order to obtain our final input-output flow matrix A. That is we let

$$A = \underline{A}^1 \mathrm{diag}(\frac{\sum_{h=1}^{N_0} \sum_{k=1}^{N_0} A^0_{h,k}}{\sum_{i=1}^{N} v_i} v) \tag{8}$$

where $\sum_{h=1}^{N_0} \sum_{k=1}^{N_0} A^0_{h,k}$ is the total WIOD output and $\mathrm{diag}(x)$ denotes the diagonal matrix whose coefficients are given by the vector x.

The initial network of supply relationships for the agent-based dynamics , Φ^0, is then obtained by normalizing the matrix A so that for all $i, j \in \mathcal{M}$, one has

$$\phi^0_{i,j} = \frac{a_{i,j}}{\sum_{k\in\mathcal{M}} a_{k,j}} \tag{9}$$

represented by the column-stochastic matrix $\Phi^t = (\phi^t_{i,j})_{i,j\in\mathcal{M}}$

4.2 General equilibrium structure

The production network defined above can be identified with the general equilibrium of a C.E.S. economy as follows.

4.2.1 household

We assume that each household h initially provides a fixed amount of labor (resp. capital) services given by $y_h := \sum_{i\in\mathcal{M}} a_{h,i}$. Furthermore, each household has C.E.S preferences of the form

$$u_i(x_h) = \left(\sum_{i\in\mathcal{F}} \beta_{h,i} x_h^\theta\right)^{1/\theta} \tag{10}$$

where for all $i \in \mathcal{M}$, $\beta_{h,i}$ is of the form $\beta_{h,i} := \gamma a_{h,i}^{1-\theta}$. Hence defined, β_h is such that the nominal demand of household h to agent i at a general equilibrium is equal to $a_{i,h}$ (when equilibrium prices are uniformly equal to one, see section 4.2.3 below).

4.2.2 firms

The production possibilities of each firm is described by a production function combining domestic labor and capital services with a C.E.S combination of domestic and international inputs. Namely, the production technology of firm j is of the form:

$$f_j(x_{w(j)}, x_{c(j)}, (x_h)_{h\in\mathcal{F}}) = x_{w(j)}^{\alpha_{w(j)}} x_{c(j)}^{\alpha_{c(j)}} \left(\sum_{h\in\mathcal{F}} \beta_{h,j} x_h^\theta\right)^{(1-\alpha_{w(j)}-\alpha_{c(j)})/\theta} \tag{11}$$

where $x_{w(j)}$ and $x_{c(j)}$ are the domestic input of labor and capital inputs, $\alpha_{w,j}$ and $\alpha_{c,j}$ are the (nominal) share of labor and capital in the input mix. The production function is calibrated by setting $\alpha_{w(j)} = \frac{a_{w(j),j}}{\sum_{i\in\mathcal{F}} a_{i,j}}$, $\alpha_{c(j)} = \frac{a_{c(j),j}}{\sum_{i\in\mathcal{F}} a_{i,j}}$ and for all $k \in \mathcal{F}$, $\beta_{k,j} = \frac{y_j^\theta}{\sum_{i\in\mathcal{F}} a_{i,j}} a_{k,j}^{1-\theta}$ where $y_j = \sum_{i\in\mathcal{M}} a_{j,i}$. Hence defined, α_j and β_j are such that the nominal demand of firm j to agent i at a general equilibrium is equal to $a_{i,h}$ (when equilibrium prices are uniformly equal to one, see section 4.2.3 below).

4.2.3 Equilibrium

We denote the economic system introduced above as $\mathcal{E}(\mathcal{M}, \alpha, \beta, \theta)$. In this setting, a general equilibrium is defined as follows.

Definition 1 *A general equilibrium of the economy $\mathcal{E}(\mathcal{M}, \alpha, \beta, \theta)$. is a collection of prices $p^* \in \mathbb{R}_+^M$, production levels $y^* \in \mathbb{R}_+^M$ and commodity flows $(x^*_{i,j})_{i,j\in\mathcal{M}} \in \mathbb{R}_+^{M\times M}$ such that:*

(i) Consumers maximize their utility under their budget constraint. That is for all $h \in \mathcal{H}$, $(y_h^*, x_h^*) \in \mathbb{R}_+ \times \mathbb{R}_+^{\mathcal{F}}$ is a solution to

$$\begin{cases} \max u_h(x) \\ s.t\ p^* \cdot x \leq p_h^* y_h^* \end{cases}$$

(ii) Firms maximize profits. That is for all $j \in \mathcal{F}$, $(y_j^*, x_j^*) \in \mathbb{R}_+ \times \mathbb{R}_+^{\mathcal{M}}$ is a solution to

$$\begin{cases} \max p_j^* y_j - p^* \cdot x_j \\ s.t\ f_j(x_j) \geq y_j \end{cases}$$

(iii) Markets clear. That is for all $i \in M$, one has

$$y_i^* = \sum_{j\in\mathcal{M}} x^*_{i,j}.$$

4.3 Agent-based dynamics

4.3.1 Optimal input combinations

The evolution of input shares specified n Equation 6 is such that firms progressively adjust their technological coefficients towards the optimal mix given their production functions. Namely, $\overline{a}^t_{\cdot,i}(p)$ is the solution of the following optimization problem

$$\begin{cases} \max & f_i\left(\frac{a_{w(i),i}}{p^t_{w(i),i}}, \frac{a_{c(i),i}}{p^t_{c(i),i}} \left(\frac{a_{j,i}}{p^t_j}\right)_{j\in\mathcal{M}}\right) \\ \text{s.t.} & \sum_{j\in\mathcal{M}} a_{j,i} = 1 \end{cases} \tag{12}$$

4.3.2 Limit properties of the dynamics

The asymptotic properties of the model, in absence of climate shocks, has extensively been analyzed in [19]. Numerical investigation reveals the presence of 3 distinct phases as illustrated in Figure 2:

(i) For very low speed of the price adjustment process (and independently of the speed of technological adjustment) the economy is characterized by a synchronized state with large "cyclical volatility". The system then oscillates between inflation and deflation, aggregate excess demand and excess supply, positive and negative profits. In this phase, as the prices evolve too slowly, output stocks carry the burden of adjustment. This leads to very strong feedback effects which entail a synchronized state of the economy

(ii) For intermediate speeds of price adjustment the system converges to equilibrium.

(iii) When both price and technological adjustment speeds are high the economy reaches an "excess demand" phase with rationing. There is persistent mismatch between supply and demand, positive inflation and sustained volatility in the network. This phase is however less robust and manifests itself only for values of θ close enough to 1.

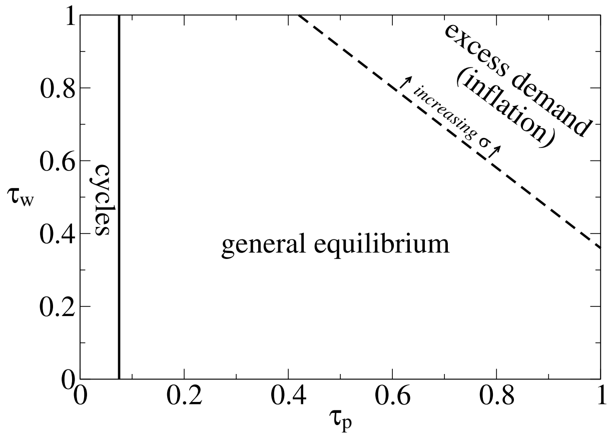

Figure 2: Phase diagram of the model with $\rho_{chg} = 0$ for $\theta = 4/5$. Note that the unstable phase in the upper right corner disappears for values of the elasticity parameter θ sufficiently smaller than 1 (see details in the text).

The equilibrium phase is largely predominant in numerical experiments. Furthermore, in the Cobb-Douglas case ($\theta = 0$), one can show analytically convergence to equilibrium if price adjustment is frictioneless($\tau_p = 1.$). Namely, one has (see [21] for the proof):

Proposition 1 *If $\theta = 0$ and $\tau_p = 1$, the only globally asymptotically stable state of the dynamical system defined by equations* (1) *to* (6) *is the element* $(\overline{m}_i, \overline{p}_i, \overline{x}_i, \overline{q}_i)_{i \in N} \in \mathbb{R}_+^N \times \mathbb{R}_+^N \times (\mathbb{R}_+^N)^N \times \mathbb{R}_+^N$ *such that:*

$$\overline{m} = A\overline{m} \tag{13}$$

$$(\overline{p}, \overline{x}, \overline{q}) \textit{ is a general equilibrium of } \mathcal{E}(\mathcal{M}, \alpha, \beta, \theta). \tag{14}$$

$$\sum_{j \in M} \overline{p}_j \overline{q}_j = \sum_{j \in M} \overline{m}_j. \tag{15}$$

Given the predominance of the equilibrium phase and the initial calibration of the model as an equilibrium of the underlying general equilibrium model, in the following, we will place ourselves in the equilibrium phase of the model, unless otherwise specified.

4.3.3 Geolocation of firms

In order to geolocalize firms in the database, we have used google maps API, by requesting for each firm in the database the spatial coordinates of all the installations of the firm in its country of incorporation.

4.4 Climate impact models

4.4.1 Climate projections

Our analysis considers chronic impacts of climate change on agricultural yields and on labor productivity as well as an array of climate-related extreme events: tropical storms, European winter storms, coastal floods, river floods, landslides, and wildfires. Consistency of the projections between these different impact domains is ensured by considering the same set of climate scenarios [rcp 2.6, rcp6 and rcp8.5, see 29], the use of climate-forcing data from the ISIMIP 2b protocol [30, 31] and the same set of climate models [by default the IPSL-CM5 Earth System Model 32]. The use of the same climate projections across domains ensure correlation between extreme events induced by climate variables (mainly temperature and precipitation) is accounted for.

4.4.2 Tropical storms

We build on the approach introduced in [33] for the projection of future impacts of tropical cyclones. We consider the whole set of historical storm tracks from IBTrACS [34] from which we generate twenty synthetic storm tracks per historical event. Future events for a given RCP scenario and year are then generated by interpolating changes in intensity and frequency from the projections in [35].

4.4.3 Winter storms

We consider as a baseline set of events the Copernicus synthetic windstorm events for Europe [36]. As for the impact of climate change, the recent literature [37, 38], finds no clear trend in frequency but mostly agrees on increasing storm intensity. Accordingly, we generate a set of future events corresponding to a given RCP scenario and year by interpolating changes in intensity derived in [39] .

4.4.4 Coastal floods

To account for the correlation between storm and coastal flooding event, we follow [40] and derive surge depths associated to storm events on the basis of a linear approximation based on wind speed [see 41]. We combine this estimate of storm-induced surge with the global topography grid at 15 arc sec derived in [42] and estimates of sea-level rise from ISIMIP2b to derive scenario and year contingent estimates of flood depth associated with each storm event.

4.4.5 River floods

We use ISIMIP multi-model global river flood model [see 43] to infer an ensemble of realisations of maximal annual flooding extent at the global scale. For each global realization, we assume that the probability of flooding at a given location is proportional to the flooded fraction in the associated cell and has a magnitude given by the associated flood depth.

4.4.6 Landslides

We infer baseline landslide risk from the atlas of global landslide and avalanche hotspots of [44]. In particular, we estimate baseline frequency of landslide event according to Table 7 in [44]. Using a parametric relation between mean annual rainfall and landslide frequency [45, 46], we then infer scenario and year contingent landslide frequency by perturbing the baseline frequency proportionally to changes in mean annual rainfall derived from ISIMIP. Beyond frequency correlation through this dependency on projected precipitations, the occurrence of each landslide event is assumed to be independent.

4.4.7 Wildfires

4.4.8 Agricultural productivity

We use projection of changes in agricultural yields from ISIMIP [47]. ISIMIP provides a multi-model ensemble.

4.4.9 Labor productivity

We infer location specific trajectories for labor productivity with a daily resolution following the approach of [48]. Namely, we build on the parametric relation established in [49] to derive Wet Bulb Globe Temperature (WBGT) from ISIMIP data on daily maximum temperature and mean relative humidity. We then use the linear approximation proposed in [48] for the effect of WBGT on labor productivity assuming a linear decrease between 25° and 39.5°. We further assume, following [50], that WBGT is increased by 3° for outdoor activities in the sun.

5 Conclusion

Acknowledgments

The authors acknowledge the financial support from the European Union's Horizon Europe research and innovation programme under the grant agreement No 101056898 DECIPHER (Decision-making framework and Processes for Holistic Evaluation of Environmental and climate policies)".

References

IPCC. Summary for policymakers. In H. O. Pörtner, D. C. Roberts, M. Tignor, E. S. Poloczanska, K. Mintenbeck, A. Alegría, M. Craig, S. Langsdorf, S. Löschke, V. Möller, A. Okem, and B. Rama, editors, Climate Change 2022: Impacts, Adaptation and Vulnerability. Contribution of Working Group II to the Sixth Assessment Report of the Intergovernmental Panel on Climate Change. Cambridge University Press, Cambridge, UK and New York, NY, USA, 2022.

Xavier Gabaix. The granular origins of aggregate fluctuations. Econometrica, 79(3):733–772, 2011.

Jean-Noël Barrot and Julien Sauvagnat. Input specificity and the propagation of idiosyncratic shocks in production networks. The Quarterly Journal of Economics, 131(3):1543–1592, 2016.

Vasco M Carvalho, Makoto Nirei, Yukiko U Saito, and Alireza Tahbaz-Salehi. Supply chain disruptions: Evidence from the great east japan earthquake. The Quarterly Journal of Economics, 136(2):1255–1321, 2021.

Daron Acemoglu, Vasco M Carvalho, Asuman Ozdaglar, and Alireza Tahbaz-Salehi. The network origins of aggregate fluctuations. Econometrica, 80(5):1977–2016, 2012.

David Rezza Baqaee and Emmanuel Farhi. The macroeconomic impact of microeconomic shocks: Beyond hulten's theorem. Econometrica, 87(4):1155–1203, 2019.

J Doyne Farmer, Cameron Hepburn, Penny Mealy, and Alexander Teytelboym. A third wave in the economics of climate change. Environmental and Resource Economics, 62:329–357, 2015.

Tomas Balint, Francesco Lamperti, Antoine Mandel, Mauro Napoletano, Andrea Roventini, and Alessandro Sapio. Complexity and the economics of climate change: a survey and a look forward. Ecological Economics, 138:252–265, 2017.

Martin L Weitzman. Fat-tailed uncertainty in the economics of catastrophic climate change. Review of Environmental Economics and Policy, 2011.

Robert S Pindyck. Climate change policy: what do the models tell us? Journal of Economic Literature, 51(3):860–872, 2013.

Jakob Zscheischler, Seth Westra, Bart JJM Van Den Hurk, Sonia I Seneviratne, Philip J Ward, Andy Pitman, Amir AghaKouchak, David N Bresch, Michael Leonard, Thomas Wahl, et al. Future climate risk from compound events. Nature Climate Change, 8(6):469–477, 2018.

William Nordhaus. A question of balance: Weighing the options on global warming policies. Yale University Press, 2014.

Simon Dietz and Nicholas Stern. Endogenous growth, convexity of damage and climate risk: how nordhaus' framework supports deep cuts in carbon emissions. The Economic Journal, 125(583):574–620, 2015.

William Nordhaus. Evolution of modeling of the economics of global warming: changes in the dice model, 1992–2017. Climatic change, 148(4):623–640, 2018.

Solomon Hsiang, Robert Kopp, Amir Jina, James Rising, Michael Delgado, Shashank Mohan, DJ Rasmussen, Robert Muir-Wood, Paul Wilson, Michael Oppenheimer, et al. Estimating economic damage from climate change in the united states. Science, 356(6345):1362–1369, 2017.

Juan-Carlos Ciscar, James Rising, Robert E Kopp, and Luc Feyen. Assessing future climate change impacts in the eu and the usa: insights and lessons from two continental-scale projects. Environmental Research Letters, 14(8):084010, 2019.

Modeling loss-propagation in the global supply network: The dynamic agent-based model acclimate. Journal of Economic Dynamics and Control, 83:232–269, 2017.

Francesco Lamperti, Giovanni Dosi, Mauro Napoletano, Andrea Roventini, and Alessandro Sapio. Faraway, so close: coupled climate and economic dynamics in an agent-based integrated assessment model. Ecological Economics, 150:315–339, 2018.

Stanislao Gualdi and Antoine Mandel. On the emergence of scale-free production networks. Journal of Economic Dynamics and Control, 73:61–77, 2016.

Antoine Mandel and Vipin P Veetil. Disequilibrium propagation of quantity constraints: Application to the covid lockdowns. Macroeconomic Dynamics, pages 1–27, 2022.

Antoine Mandel and Vipin P Veetil. Monetary dynamics in a network economy. Journal of Economic Dynamics and Control, 125:104084, 2021.

Robert Axtell. The complexity of exchange. The Economic Journal, 115(504):F193–F210, 2005.

Tiziano Squartini, Guido Caldarelli, Giulio Cimini, Andrea Gabrielli, and Diego Garlaschelli. Reconstruction methods for networks: The case of economic and financial systems. Physics reports, 757:1–47, 2018.

Erik Dietzenbacher, Bart Los, Robert Stehrer, Marcel Timmer, and Gaaitzen De Vries. The construction of world input–output tables in the wiod project. Economic systems research, 25(1):71–98, 2013.

Antoine Mandel and Vipin Veetil. The economic cost of covid lockdowns: an out-of-equilibrium analysis. Economics of Disasters and Climate Change, 4:431–451, 2020.

Marcel P Timmer, Erik Dietzenbacher, Bart Los, Robert Stehrer, and Gaaitzen J De Vries. An illustrated user guide to the world input–output database: the case of global automotive production. Review of International Economics, 23(3):575–605, 2015.

Carissa Holler Phillips. S&p capital iq. Journal of Business & Finance Librarianship, 17(3):279–286, 2012.

Sabina Dewan, Ekkehard Ernst, and Souleima Achkar Hilal. World employment and social outlook: trends 2022. ILO, Geneva, Switzerland, 2022.

Richard H Moss, Jae A Edmonds, Kathy A Hibbard, Martin R Manning, Steven K Rose, Detlef P Van Vuuren, Timothy R Carter, Seita Emori, Mikiko Kainuma, Tom Kram, et al. The next generation of scenarios for climate change research and assessment. Nature, 463(7282):747–756, 2010.

Lila Warszawski, Katja Frieler, Veronika Huber, Franziska Piontek, Olivia Serdeczny, and Jacob Schewe. The inter-sectoral impact model intercomparison project (isi–mip): project framework. Proceedings of the National Academy of Sciences, 111(9):3228–3232, 2014.

Katja Frieler, Stefan Lange, Franziska Piontek, Christopher PO Reyer, Jacob Schewe, Lila Warszawski, Fang Zhao, Louise Chini, Sebastien Denvil, Kerry Emanuel, et al. Assessing the impacts of 1.5 c global warming–simulation protocol of the inter-sectoral impact model intercomparison project (isimip2b). Geoscientific Model Development, 10(12):4321–4345, 2017.

J-L Dufresne, M-A Foujols, Sébastien Denvil, Arnaud Caubel, Olivier Marti, Olivier Aumont, Yves Balkanski, Slimane Bekki, Hugo Bellenger, Rachid Benshila, et al. Climate change projections using the ipsl-cm5 earth system model: from cmip3 to cmip5. Climate dynamics, 40:2123–2165, 2013.

Gabriela Aznar-Siguan and David N Bresch. Climada v1: a global weather and climate risk¡? xmltex\break?¿ assessment platform. Geoscientific Model Development, 12(7):3085–3097, 2019.

Kenneth R Knapp, Michael C Kruk, David H Levinson, Howard J Diamond, and Charles J Neumann. The international best track archive for climate stewardship (ibtracs) unifying tropical cyclone data. Bulletin of the American Meteorological Society, 91(3):363–376, 2010.

Thomas R Knutson, Joseph J Sirutis, Ming Zhao, Robert E Tuleya, Morris Bender, Gabriel A Vecchi, Gabriele Villarini, and Daniel Chavas. Global projections of intense tropical cyclone activity for the late twenty-first century from dynamical downscaling of cmip5/rcp4. 5 scenarios. Journal of Climate, 28(18):7203–7224, 2015.

Copernicus Climate Change Service. Synthetic windstorm events for europe from 1986 to 2011, 2022. Database.

IPCC. Climate Change 2021: The Physical Science Basis. Contribution of Working Group I to the Sixth Assessment Report of the Intergovernmental Panel on Climate Change. Cambridge University Press, Cambridge, UK and New York, NY, USA, 2021.

Frauke Feser, M Barcikowska, O Krueger, Frederik Schenk, R Weisse, and L Xia. Storminess over the north atlantic and northwestern europe—a review. Quarterly Journal of the Royal Meteorological Society, 141(687):350–382, 2015.

Tobias Pardowitz. Anthropogenic changes in the frequency and severity of European winter storms: mechanisms, impacts and their uncertainties. PhD thesis, Frei University Berlin, 2015.

Arun Rana, Qinhan Zhu, Annette Detken, Karina Whalley, and Christelle Castet. Strengthening climate-resilient development and transformation in viet nam. Climatic Change, 170(1-2):4, 2022.

Liming Xu. A simple coastline storm surge model based on pre-run slosh outputs. In 29th Conference on Hurricanes and Tropical Meteorology, 2010.

Brook Tozer, David T Sandwell, Walter HF Smith, C Olson, JR Beale, and P Wessel. Global bathymetry and topography at 15 arc sec: Srtm15+. Earth and Space Science, 6(10):1847–1864, 2019.

Francesco Dottori, Wojciech Szewczyk, Juan-Carlos Ciscar, Fang Zhao, Lorenzo Alfieri, Yukiko Hirabayashi, Alessandra Bianchi, Ignazio Mongelli, Katja Frieler, Richard A Betts, et al. Increased human and economic losses from river flooding with anthropogenic warming. Nature Climate Change, 8(9):781–786, 2018.

Farrokh Nadim, Oddvar Kjekstad, Pascal Peduzzi, Christian Herold, and Christian Jaedicke. Global landslide and avalanche hotspots. Landslides, 3:159–173, 2006.

DL Hicks. A way to estimate the frequency of rainfall-induced mass movements (note). Journal of Hydrology (New Zealand), pages 59–67, 1995.

Michael J Crozier. Deciphering the effect of climate change on landslide activity: A review. Geomorphology, 124(3-4):260–267, 2010.

Christoph Müller, Joshua Elliott, David Kelly, Almut Arneth, Juraj Balkovic, Philippe Ciais, Delphine Deryng, Christian Folberth, Steven Hoek, Roberto C Izaurralde, et al. The global gridded crop model intercomparison phase 1 simulation dataset. Scientific data, 6(1):50, 2019.

Shouro Dasgupta, Nicole van Maanen, Simon N Gosling, Franziska Piontek, Christian Otto, and Carl-Friedrich Schleussner. Effects of climate change on combined labour productivity and supply: an empirical, multi-model study. The Lancet Planetary Health, 5(7):e455–e465, 2021.

Roland Stull. Wet-bulb temperature from relative humidity and air temperature. Journal of applied meteorology and climatology, 50(11):2267–2269, 2011.

T Kjellstrom, B Lemke, M Otto, O Hyatt, K Dear, et al. Occupational heat stress: contribution to who project on “global assessment of the health impacts of climate change”, which started in 2009. Mapua: Health and Environment International Trust, 4, 2014.